Track Finding and TOF Particle Identification with various TPC Pad-row Patterns

Pablo Yepes
Physics Department, Rice University, Houston TX 77251-1892

March 24, 1995

1 Introduction

The STAR Time Projection Chamber (TPC) provides tracking information in three dimensions in a large phase space. Unfortunately these data only become available for online event selection at the third level trigger (L3). The raw information provided by the detector will be converted into space points by microprocessors. The number and computer power of these devices determines the number of space points that will be available for the L3 tracking algorithms. At this time it is not certain whether enough processors to treat all the TPC information will be available. Therefore it is very important to study how the pattern recognition performs with only partial TPC information.

2 Data sample

A sample of 10 central Lund AuAu events were used to study the performance with heavy ion interactions. In addition a sample of 2000 tracks with a flat distribution in p_t in the range 0-40 GeV was also utilized.

Events were run through the STAR GEANT simulation. The output was treated with the standard STAR analysis shell (TAS). TPC space points were generated with the fast tpc simulator (tfs). The track finding was performed with the trigger package rft. In addition the TOF particle identification code was utilized in the reconstruction chain.

3 Pad-row Configurations

The following scenarios concerning the available TPC pad-rows were considered:

1. Full TPC

2. Pad-rows 21-45

3. Pad-rows 30-45

4. Even Pad-rows

5. Third Pad-rows: Pad-rows multiple of 3.

The fast pattern recognition has the possibility of considering tracks as coming from the primary vertex in the plane perpendicular to the beam. This option will be referred to as vertex constraint. In fact the primary vertex position is not calculated since it needs tracking information not available at that stage. The program considers all tracks being originated at a fixed point (0,0). This approximation should be good enough in realistic conditions since the transverse beam dispersion is less than a milimiter. The vertex constraint makes the pattern recognition algorithms simpler. However this option has a serious drawback. This is the lost of all information concerning tracks coming from secondary vertices, since they are forced to pass through the primary vertex.

4 Reconstruction efficiency

Track reconstruction efficiency was estimated using high quality tracks, defined as those that are produced at the primary vertex and generate at least 20 space points in the TPC. The reconstruction efficiency is defined as the fraction of those *good quality tracks* that are found by the pattern recognition program and that more than 90% of the space points assigned to the track were generated by it.

Figure 1 shows the track reconstruction efficiency as a function of transverse momentum, p_T, for the five configurations considered with and without vertex constraint. As can be expected, the efficiency deteriorates when the number of pad-rows decreases.

Figure 2 shows the the track reconstruction efficiency as a function of rapidity, η, for the various configurations.

Figure 3 shows the momentum resolution as a function of transverse p_t obtained with the various pad-row configurations for central Lund AuAu events. The momentum resolution was obtained by fitting a gaussian to the relative difference between the real and the measured momentum in the various p_t intervals. As can be observed, the resolution obtained when only pad-rows 21-45 or 30-45 are used without vertex constraint is rather poor. The rest of the distributions look rather similar, especially for the full TPC with even and third pad-rows. Table 6 contains the momentum resolution integrated over p_t.

The momentum resolution as a function of p_t in a larger range in transverse momentum is shown in Figure 4. The results shown were obtained from a sample of events with tracks generated with a flat distribution in the p_t range 0-40 GeV. The momentum resolution was obtained from the comparison of reconstructed and generated momenta. The dispersion of the distributions, rather that a gaussian fit, was taken as the momentum resolution, since some distributions are not gaussian. In this case the results

corresponding to pad-rows 21-45 and 30-45 without vertex constraint were not plotted since they are very poor. The other configurations yield rather similar results.

5 TOF Particle Identification

Track reconstruction at the third level trigger will allow particle identification (PID). Two complementary methods are used in STAR for PID: dE/dx measurements (TPC and SVT) and time of flight techniques with the TOF detector. The dE/dx study of the PID capabilities at L3 requires a detailed simulation of cluster formation and finding. This is outside the scope of the present analysis. Therefore only the TOF PID capabilities will be investigated.

Two quantities enter in the determination of the particle mass with a TOF detector: the trajectory length and time of flight. In order to understand how PID will behave at L3, the resolution in the determination of those two quantities was studied for the different pad-row configurations.

Figure 5 shows the difference between the real track length and the value obtained from the reconstruction. As in previous distributions, the measurement of the track length deteriorates when only short pad-row configurations (21-45 and 30-45) with no vertex are used. However the vertex inclusion improves the resolution substantially. Using even or third pad-rows gives quite acceptable results even without the vertex constraint. Table 6 contains the numerical values of the length resolutions obtained by fitting gaussians to the distributions.

Figure 6 shows the time of flight resolution for the different configurations. It is to be noted that the time resolution depends on the tracking quality. This is due to the correction applied to the raw time provided by the TOF. This correction is a function of the distance of the particle impact in the TOF counter to the its photo-multiplier. The quality of the tracking will determine the accuracy in the impact measurement. As can be observed, the time resolution does not seem to depend on the vertex constraint presence. In addition configuration 21-45 and 30-45 give better results than even and third rows. This is not difficult to understand since the more information available in the region close to the TOF the better the track hit position will be. Table 6 contains the numerical values of the time resolutions obtained by fitting gaussians to the distributions.

Figure 7 shows the particle mass distribution, m, obtained combining tracking with TOF information in the range $0.2 < m < 1.2$ GeV. Tracks were required to be long enough (>20 pad-rows for the full TPC, even rows and third rows and >10 for the other configurations). The kaon and proton peaks are clearly visible except for the configurations 21-45 and 30-45 with no vertex. However when the vertex is included clear signals can be observed for all configurations. This plot shows that particle identification with the TOF at L3 should be possible.

	$\Delta p/p$ (%)	Length Resolution (cm)	Time Resolution (ps)	CPU time (sg)
No vertex				
Full TPC	2.1	0.8	90	33.3
Pad-rows 21-45	7.5	1.2	86	13.5
Pad-rows 30-45	13.7	2.9	91	9.2
Even Pad-rows	2.5	0.9	94	18.6
Third Pad-rows	2.8	1.0	112	15.6
Vertex				
Full TPC	2.9	0.8	90	36.8
Pad-rows 21-45	2.2	1.1	90	14.1
Pad-rows 30-45	2.2	1.4	92	9.4
Even Pad-rows	3.0	0.9	95	18.3
Third Pad-rows	2.9	1.0	114	14.8

Table 1: Momentum, Track length and time of flight resolutions for the different pad-row configurations considered.

6 Timing

Table 6 shows the mean time necessary to reconstruct a central AuAu event on an IBM RISC 6000/370. The program reconstructs an average number of tracks ranging from 2677 (Full TPC with vertex) to 1672 (Third rows without vertex). Reconstruction times are for the whole event. Due to the program logic, no large improvements are expected if the event is split in sectors.

7 Conclusions

The tracking performance with various pad-row patterns has been studied. No dramatic differences among them have been found when the vertex is included as a constraint. The vertex inclusion seems to have beneficial effects for reduced pad-row configurations. However information about secondary vertices, which may be very useful for triggering on strangeness, is lost. In addition particle identification with the TOF has been shown to be possible even in the case with only the 16 outer most pad-rows.

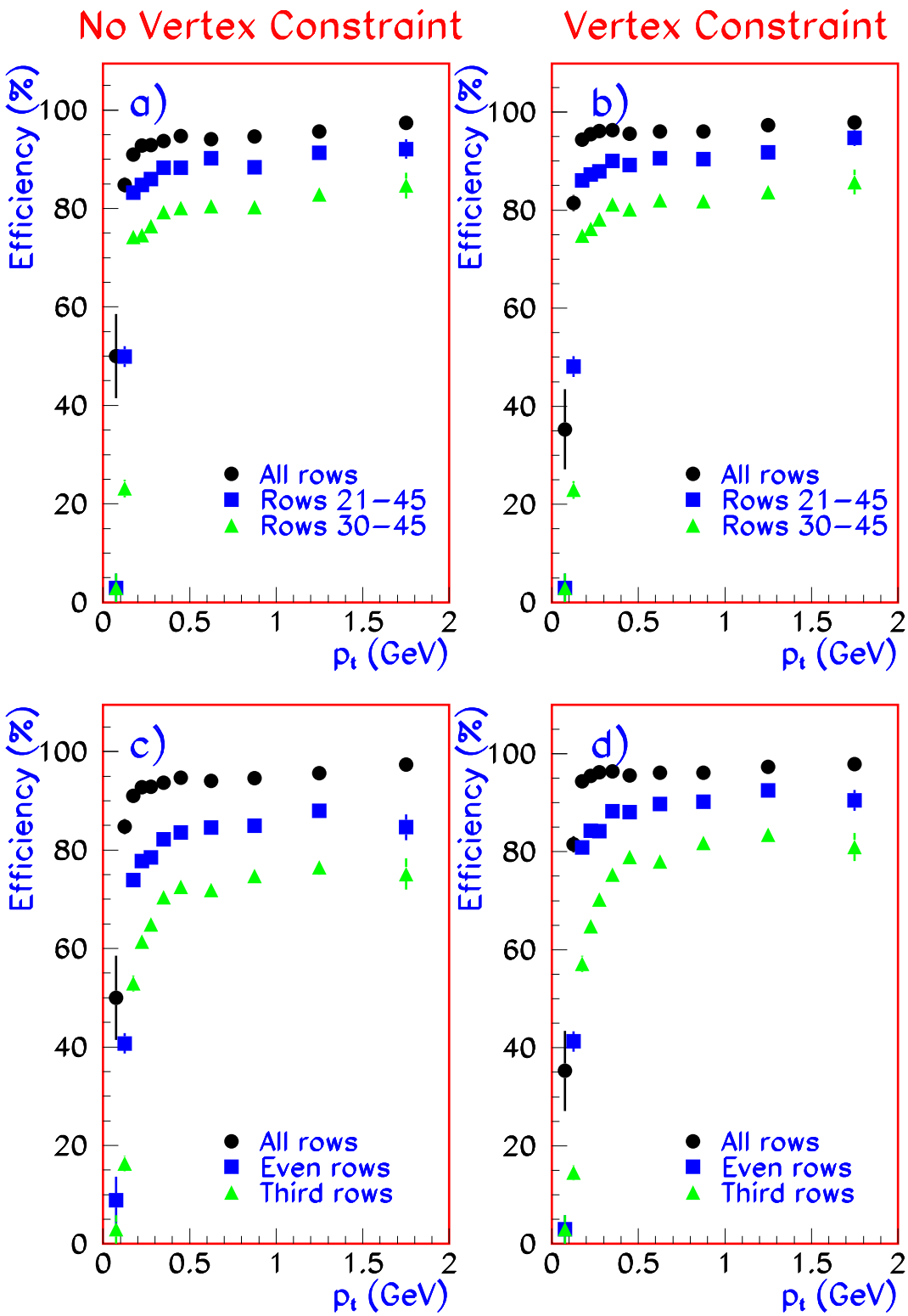

Figure 1: Track finding efficiency as a function of p_T for (a)-(b) full TPC, pad-rows 21-45 and 30-45 with and without vertex constraint and (c)-(d) full TPC, even pad-rows and multiple of 3 pad-rows with and without vertex constraint.

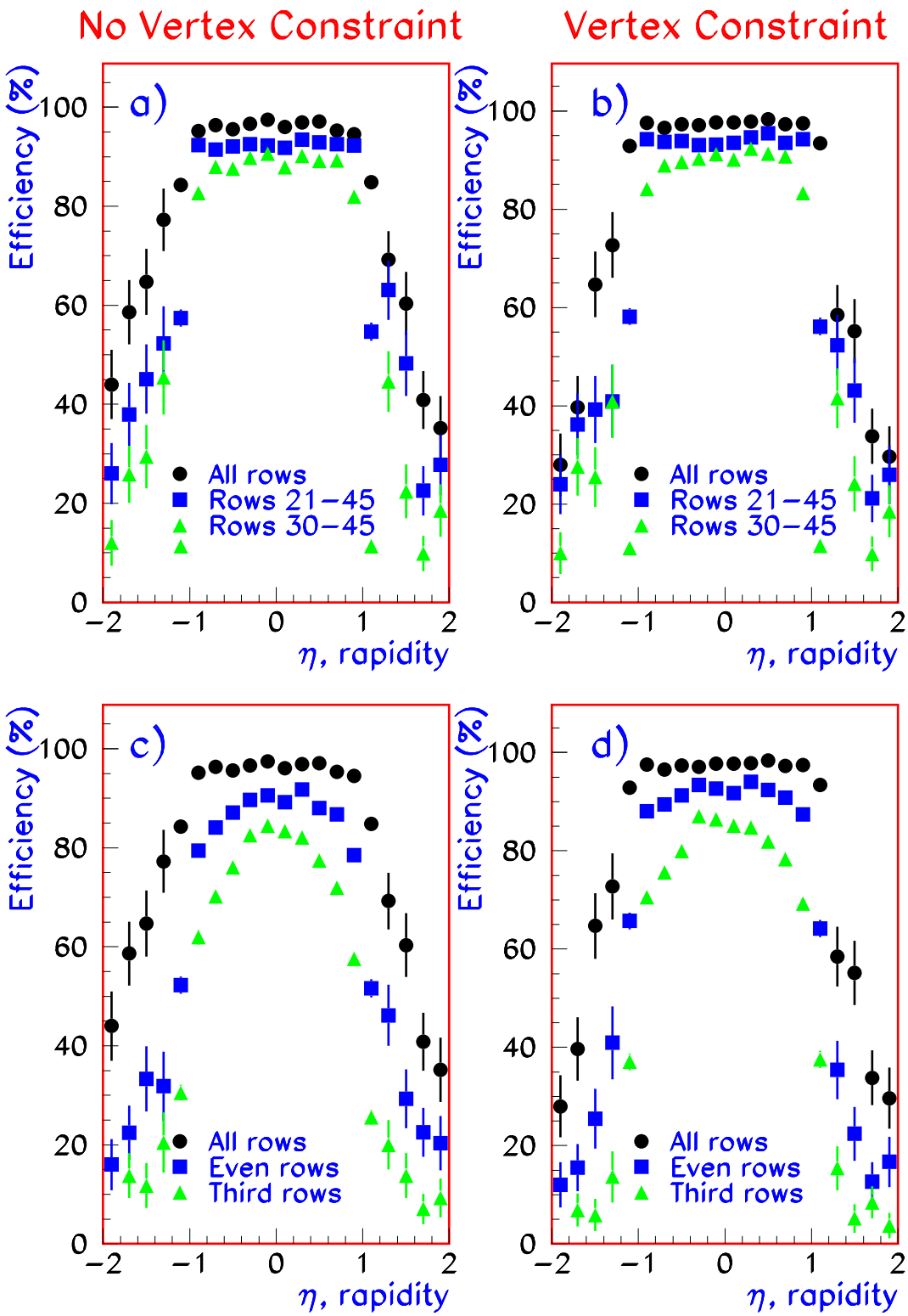

Figure 2: Track finding efficiency as a function of η for (a)-(b) full TPC, pad-rows 21-45 and 30-45 with and without vertex constraint and (c)-(d) full TPC, even pad-rows and multiple of 3 pad-rows with and without vertex constraint.

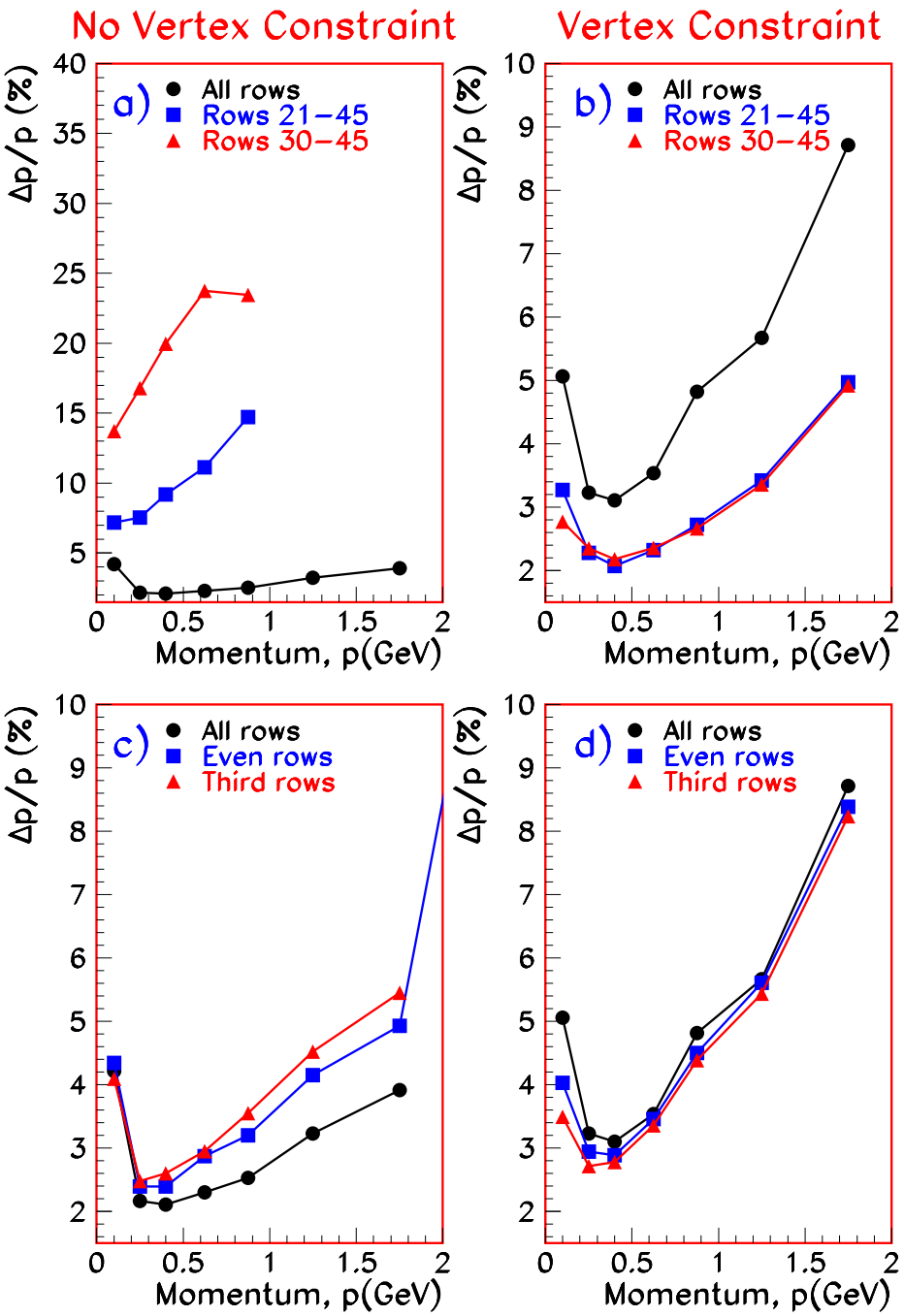

Figure 3: Momentum resolution as a function of p_t for (a)-(b) full TPC, pad-rows 21-45 and 30-45 with and without vertex constraint and (c)-(d) full TPC, even pad-rows and multiple of 3 pad-rows with and without vertex constraint.

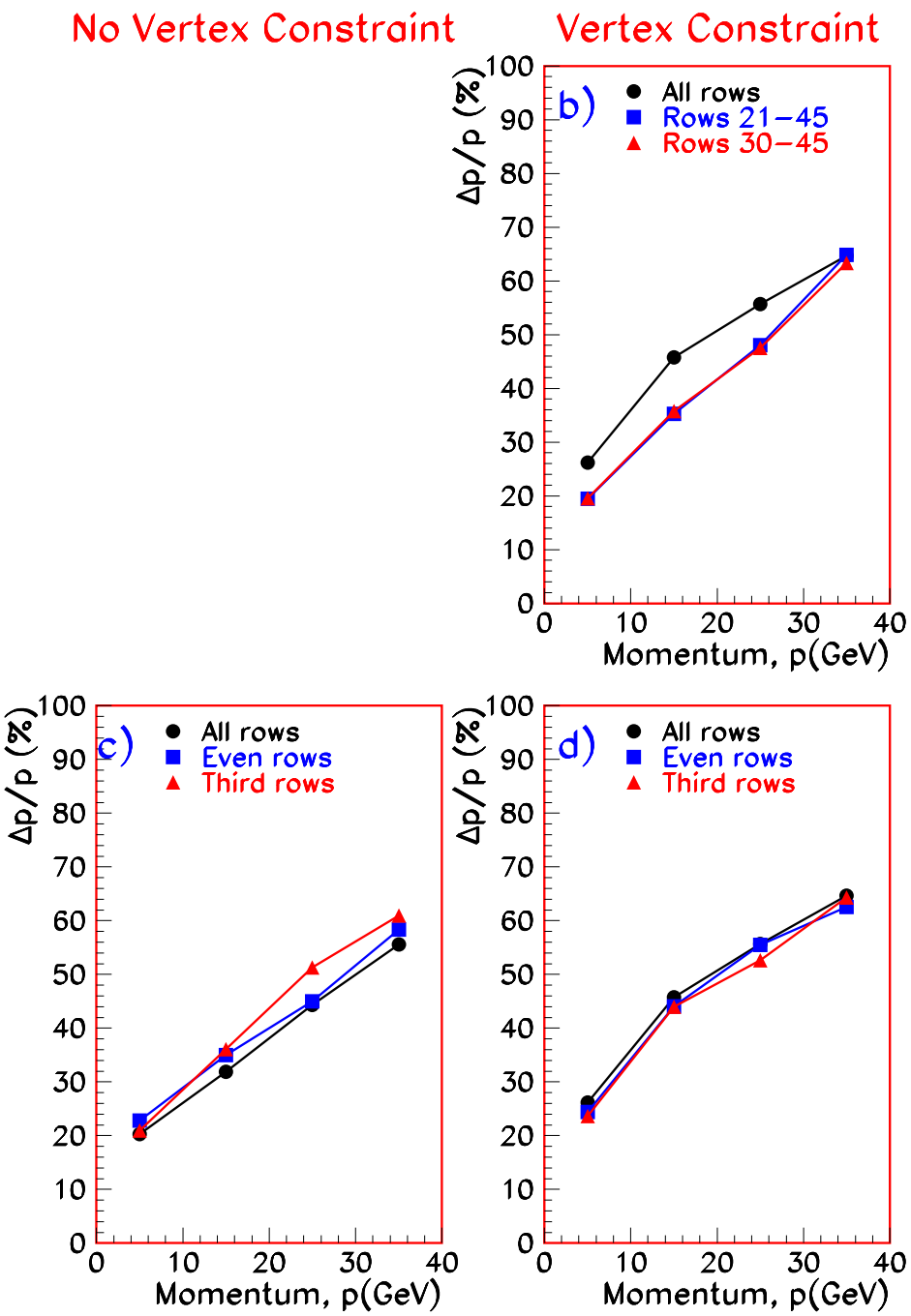

Figure 4: Momentum resolution as a function of p_t for (a)-(b) full TPC, pad-rows 21-45 and 30-45 with and without vertex constraint and (c)-(d) full TPC, even pad-rows and multiple of 3 pad-rows with and without vertex constraint.

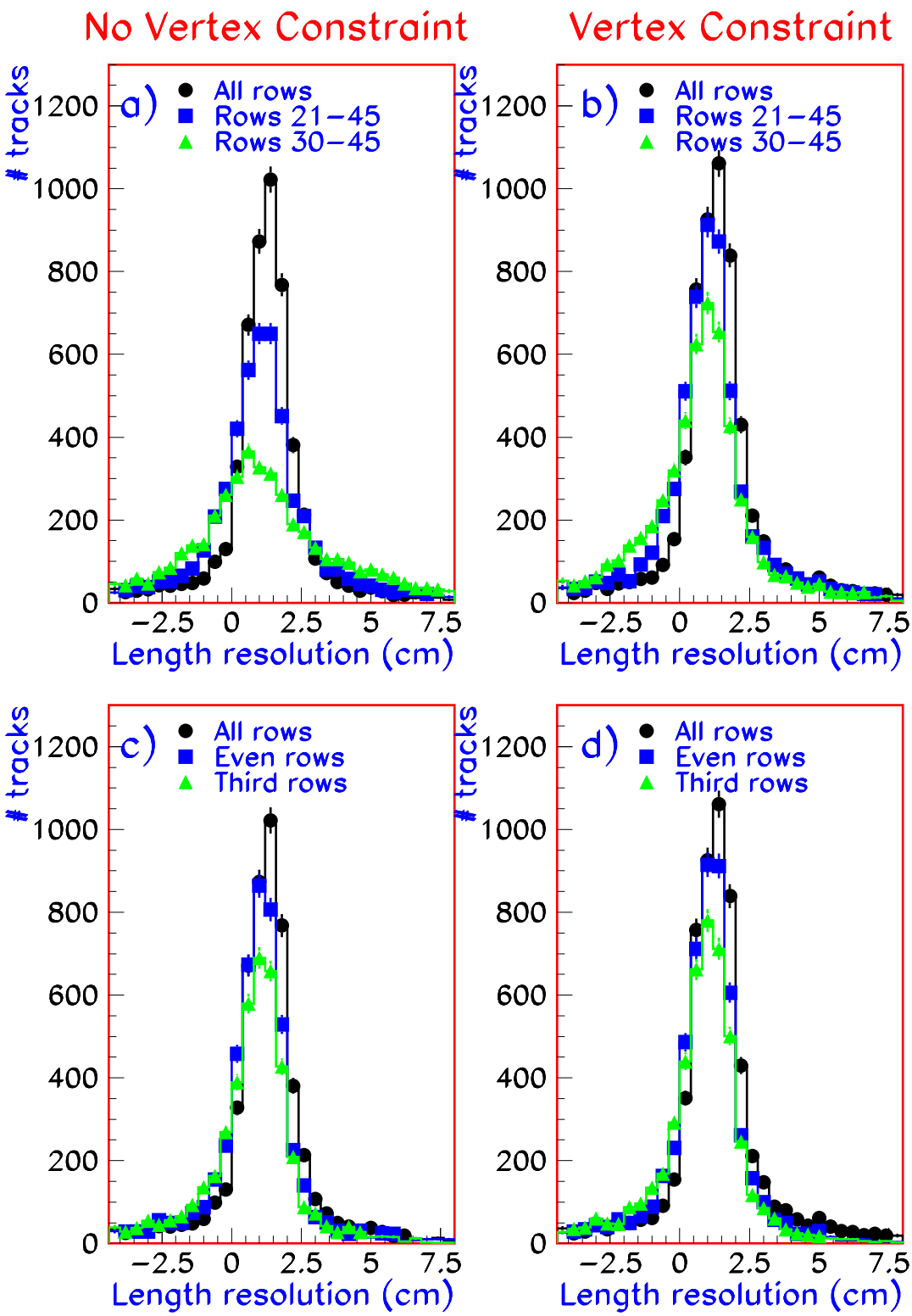

Figure 5: Track length resolution for (a)-(b) full TPC, pad-rows 21-45 and 30-45 with and without vertex constraint and (c)-(d) full TPC, even pad-rows and multiple of 3 pad-rows with and without vertex constraint.

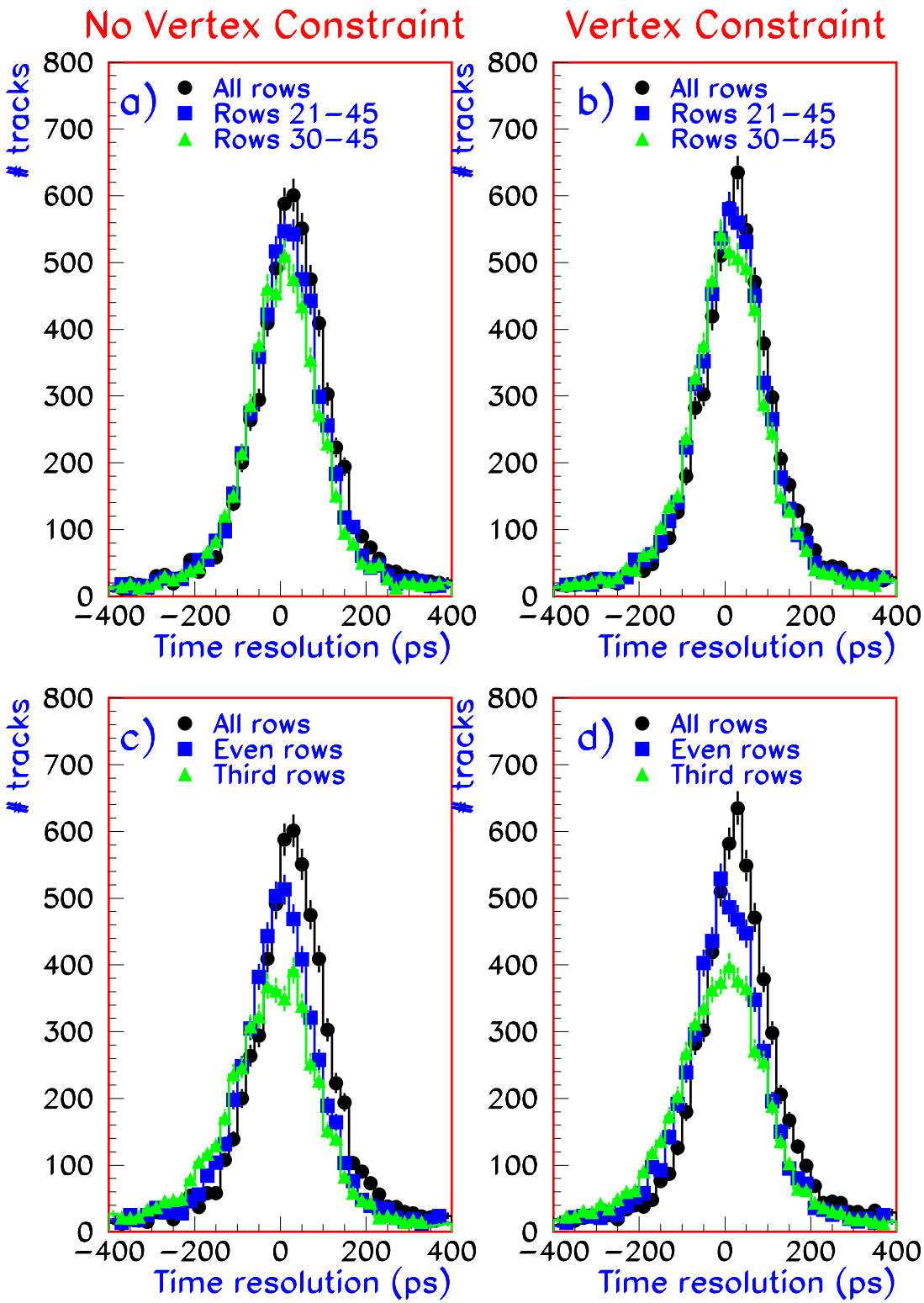

Figure 6: Time resolution for (a)-(b) full TPC, pad-rows 21-45 and 30-45 with and without vertex constraint and (c)-(d) full TPC, even pad-rows and multiple of 3 pad-rows with and without vertex constraint.

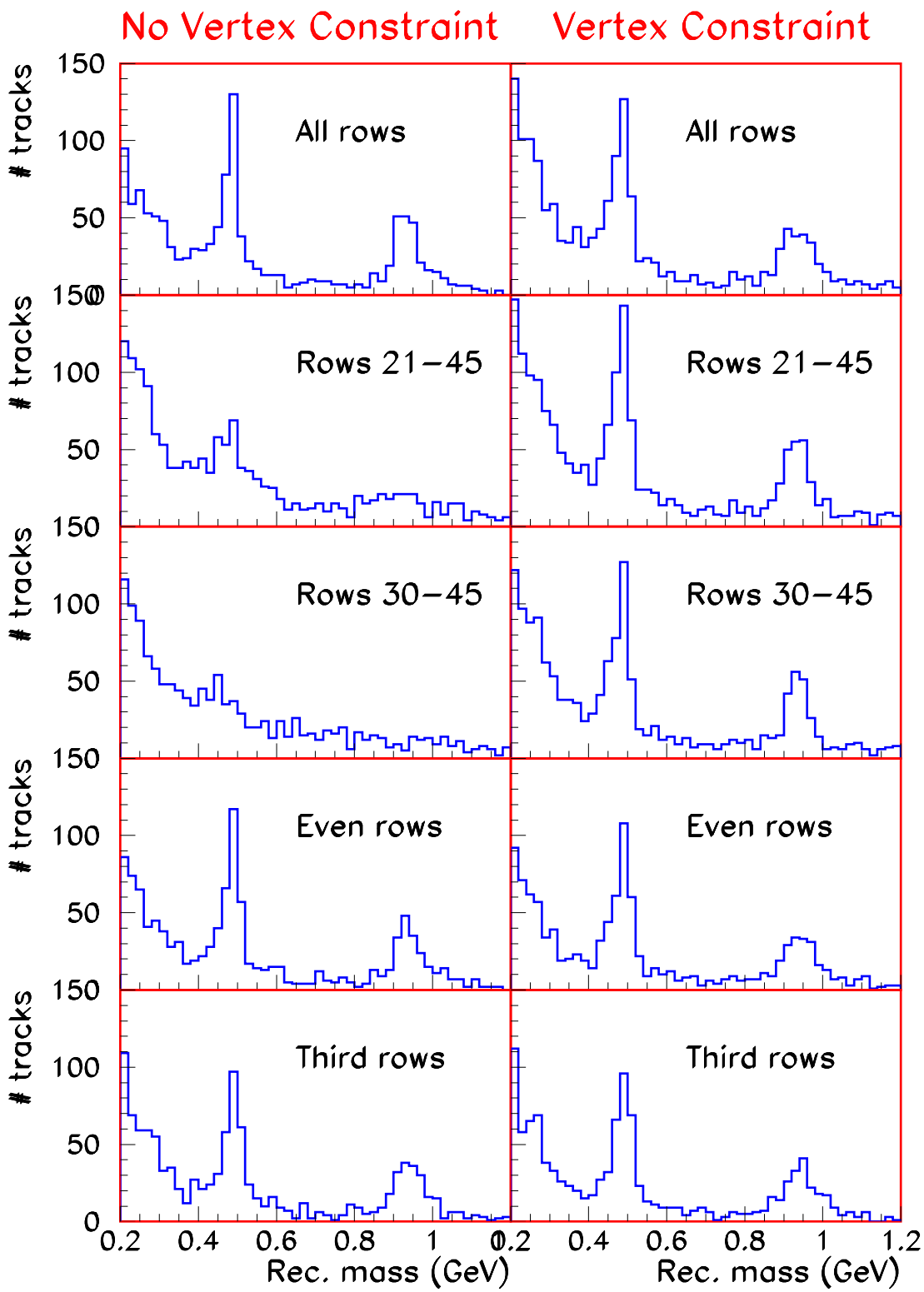

Figure 7: Particle mass spectra obtained with the fast tracking and TOF full TPC, pad-rows 21-45 and 30-45, even pad-rows and third pad-rows with and without vertex constraint.